Journal of
Plankton Research

plankt.oxfordjournals.org

J. Plankton Res. (2014) 36(3): 641–657. First published online January 7, 2014 doi:10.1093/plankt/fbt125

Impact of CO_2 enrichment on organic matter dynamics during nutrient induced coastal phytoplankton blooms

ANJA ENGEL[1,2]*, JUDITH PIONTEK[1,2], HANS-PETER GROSSART[3,4], ULF RIEBESELL[1], KAI G. SCHULZ[1,5] AND MARTIN SPERLING[1,2]

[1]GEOMAR HELMHOLTZ CENTRE FOR OCEAN RESEARCH KIEL, KIEL 24105, GERMANY, [2]ALFRED WEGENER INSTITUTE FOR POLAR AND MARINE RESEARCH, AM HANDELSHAFEN 12, BREMERHAVEN 27570, GERMANY, [3]DEPARTMENT EXPERIMENTAL LIMNOLOGY, IGB-NEUGLOBSOW, ALTE FISCHERHUETTE 2, STECHLIN 16775, GERMANY, [4]INSTITUTE FOR BIOCHEMISTRY AND BIOLOGY, POTSDAM UNIVERSITY, MAULBEERALLEE 2, POTSDAM 14469, GERMANY AND [5]CENTRE FOR COASTAL BIOGEOCHEMISTRY, SCHOOL OF ENVIRONMENTAL SCIENCE AND MANAGEMENT, SOUTHERN CROSS UNIVERSITY, PO BOX 157, LISMORE, NSW 2480, AUSTRALIA

*CORRESPONDING AUTHOR: aengel@geomar.de

Received August 7, 2013; accepted November 21, 2013

Corresponding editor: Zoe Finkel

A mesocosm experiment was conducted to investigate the impact of rising fCO_2 on the build-up and decline of organic matter during coastal phytoplankton blooms. Five mesocosms (~38 m^3 each) were deployed in the Baltic Sea during spring (2009) and enriched with CO_2 to yield a gradient of 355–862 μatm. Mesocosms were nutrient fertilized initially to induce phytoplankton bloom development. Changes in particulate and dissolved organic matter concentrations, including dissolved high-molecular weight (>1 kDa) combined carbohydrates, dissolved free and combined amino acids as well as transparent exopolymer particles (TEP), were monitored over 21 days together with bacterial abundance, and hydrolytic extracellular enzyme activities. Overall, organic matter followed well-known bloom dynamics in all CO_2 treatments alike. At high fCO_2, higher ΔPOC:ΔPON during bloom rise, and higher TEP concentrations during bloom peak, suggested preferential accumulation of carbon-rich components. TEP concentration at bloom peak was significantly related to subsequent sedimentation of particulate organic matter. Bacterial abundance increased during the bloom and was highest at high fCO_2. We conclude that increasing fCO_2 supports production and exudation of carbon-rich components, enhancing particle aggregation and settling, but also providing substrate and attachment sites for bacteria. More labile organic carbon and higher bacterial abundance can increase rates

available online at www.plankt.oxfordjournals.org

of oxygen consumption and may intensify the already high risk of oxygen depletion in coastal seas in the future.

KEYWORDS: mesocosm; ocean acidification; phytoplankton; organic matter; TEP

INTRODUCTION

The uptake of anthropogenic CO_2 by the ocean and the subsequent acidification of seawater have recently gathered attention in marine research. Multiple effects of changes in pH and CO_2 concentration are expected for marine organisms, their physiological rates, species diversity and population dynamics, in turn affecting productivity and biogeochemical cycling in ecosystems (Kroeker *et al.*, 2010; Liu *et al.*, 2010; Riebesell and Tortell, 2011; Gehlen *et al.*, 2011). Experimental studies have suggested that a higher assimilation of carbon into organic matter at high CO_2 may increase extracellular organic matter release from phytoplankton cells (Engel, 2002; Kim *et al.*, 2011; Borchard and Engel, 2012). As a consequence, concentrations of labile dissolved organic carbon (DOC) could rise, potentially affecting marine ecosystem structure and microbial re-mineralization rates. Rising CO_2 has furthermore been shown to cause selective enrichment of carbon in particulate organic matter (POM) during phytoplankton bloom and post-bloom periods (Engel *et al.*, 2005; Riebesell *et al.*, 2007; Bellerby *et al.*, 2008) and may favour a higher sequestration of organic carbon to deeper waters or to the seafloor. Oxygen utilization in marine systems is directly related to the availability of labile organic carbon, and an enhanced microbial draw-down of oxygen in deeper waters, eventually expanding marine anoxia, has been suggested as a possible indirect effect of ocean acidification (Oschlies *et al.*, 2008).

One link between a CO_2-enhanced extracellular release of organic carbon in the surface ocean and a higher carbon content of particles settling to depth is transparent exopolymer particles (TEP). TEP form from dissolved carbohydrates, are therefore carbon-rich and induce the formation of particle aggregates, potentially enhancing export fluxes (Alldredge *et al.*, 1993; Engel and Passow, 2001; Passow, 2002). TEP also provide habitat and substrate to marine bacteria and stimulate the microbial processing of organic matter (Simon *et al.*, 2002). Due to their large specific surface area and high physicochemical reactivity, TEP furthermore play an important role in trace metal cycling, specifically in coastal areas subject to land-based metal emission (Mari *et al.*, 2009).

In contrast to surface waters of the open ocean with a relatively stable pH, marine phyto- and bacterioplankton in coastal and estuarine regions are exposed to pronounced CO_2 and pH fluctuations on a seasonal scale (Hofmann *et al.*, 2011). Boknis Eck (54.53°N, 10.03°E) is a coastal monitoring site in the Kiel Bight, South-Western Baltic Sea, and monitored on a monthly basis since 1957 for the surveillance of several chemical and biological components (Fig. 1). Time-series measurements of pH at Boknis Eck are available for the period of 1986–1998 and exhibit strong seasonality (Fig. 2). While pH values down to 7.57 are observed in surface waters (0–5 m) after water-column mixing in autumn and winter, biological activity greatly reduces CO_2 concentration during the spring bloom, raising pH up to 8.6 in the period April to August. Thus, pH at this site is highly variable and occasionally as low as predicted for the future open ocean. The high seasonal pH variability in the Baltic Sea is partly due to the relatively low seawater buffering capacity and typical for brackish systems having a lower salinity (0.5–24.7; Leppäranta and Myrberg, 2009) and lower alkalinity than the open ocean (Omstedt *et al.*, 2010). At Boknis Eck, a halocline at about 15 m results from the inflow of North Sea seawater. Strong water-column stratification, therefore, prevents deeper water from equilibration with the atmosphere and promotes the accumulation of CO_2 as the end-product of organic matter mineralization over the summer months. Vertical mixing during autumn/winter then leads to the entrainment of CO_2- and nutrient rich bottom water to the surface and supports biological production during late winter/early spring. As a consequence, the partial pressure of CO_2 in surface waters at Boknis Eck varies between 200 and 4000 μatm over the annual cycle (Melzner *et al.*, 2012). Superimposed, photosynthesis and microbial respiration result in daily variations in seawater pH and CO_2 concentration (Schulz and Riebesell, 2012).

It can be expected that coastal, pelagic ecosystems, like the Boknis Eck system, include organisms that are adapted to and tolerate variations in pH and in CO_2 concentration. Investigating this ecosystem can therefore provide a clue as to how plankton may respond to future CO_2/pH levels, but also may provide insight into the present day's impacts of low pH/high CO_2 pulses that readily occur in coastal seas.

So far, little is known about how anthropogenic changes influence organic matter dynamics in coastal seas. Using an *in-situ* perturbation experiment, this study shows how an increase in seawater fCO_2 and the related

decline in pH can affect the build-up and decline of particulate and dissolved organic matter during nutrient induced bloom periods. The CO_2 levels applied during this study ranged between 355 and 862 μatm and thus are representative of the present day coastal and expected future open ocean conditions as estimated by modelling studies (Feely *et al.*, 2009; Omstedt *et al.*, 2009).

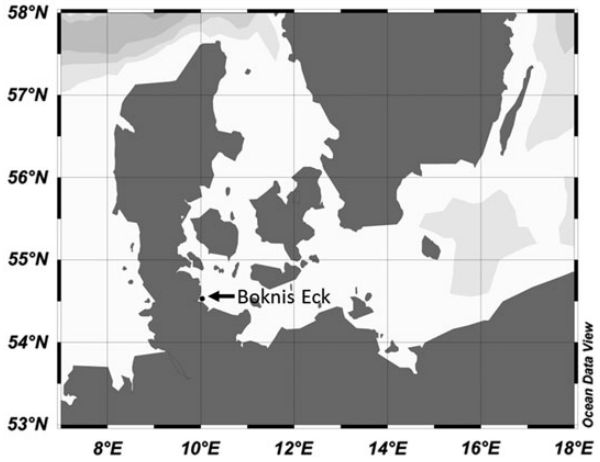

Fig. 1. Map of the location, Boknis Eck, in Kiel Bight at about 54.53°N, 10.03°E, where the mesocosms were deployed during spring (2009).

METHOD

Set-up of mesocosm experiment

The mesocosm study was conducted in spring 2009 (20 May to 5 July, 2009) in the coastal western Baltic Sea (Boknis Eck in Kiel Bight at about 54.53°N, 10.03°E) (Fig. 1). The set-up of the experiment and the design of the Kiel Off-Shore Mesocosms for future Ocean Simulations (KOSMOS) are given in more detail by Schulz and Riebesell (Schulz and Riebesell, 2012). Briefly, six mesocosms (13.5 m long, 2 m wide) made of thermoplastic polyurethane (TPU) were moored at about 1 nautical mile distance from the shoreline (Fig. 3). Bags were flushed in vertical position with open bottom and top, the later being underneath the water surface, for 2 days to ensure homogeneity of enclosed water masses. Then, mesocosms were closed by pulling the top end above the surface and closing the bottom with two flaps by divers (see Riebesell *et al.*, 2013 for details).

CO_2 was added to five mesocosms, while one mesocosm (M2) was left unperturbed and served as a control. CO_2 manipulation was conducted gradually over 3 days (d_0, d_1, d_3) by injections of 25–155 L CO_2-enriched, filtered (<20 μm) seawater, collected previously at the mooring site. The CO_2-enriched seawater was pumped through a dispersal device that was lowered to 12 m depth and pulled up again to the surface several times, evenly distributing the CO_2 addition between 0 and

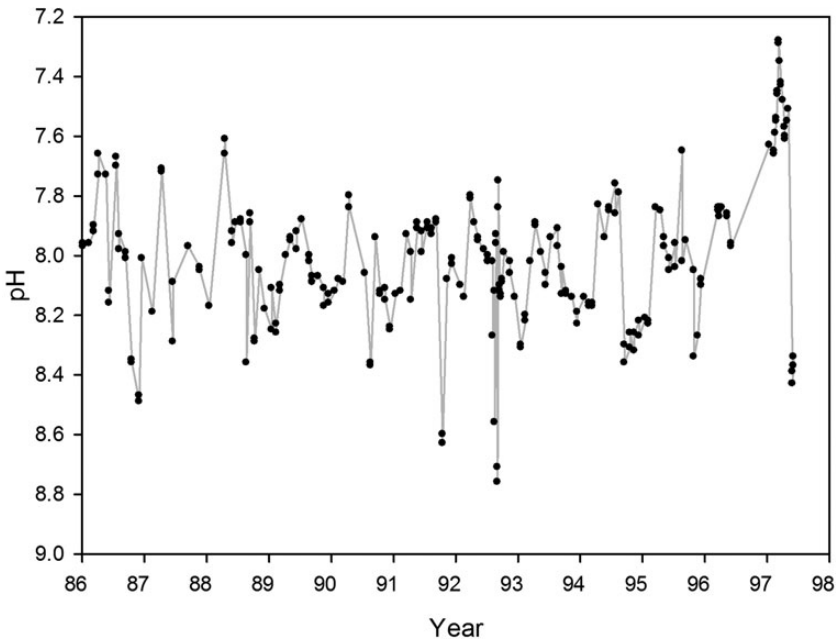

Fig. 2. pH over a period of 10 years (1986–1997) in surface waters (0–5 m depth) at the monitoring station Boknis Eck (coastal Baltic Sea), near by the site of the mesocosm experiment, exhibiting annual variations in the range 7.4–8.91.

Fig. 3. Floating KOSMOS in the coastal Baltic Sea in spring 2009.

12 m. In this way, a CO_2 gradient was established in the mesocosm ensemble, spanning initially 355 (M2) to 862 (M6) μatm. Applying a gradient of treatments rather than aiming for treatment replication is a viable approach with no loss of statistical power at limited possible replicates as in this study (Havenhand *et al.*, 2011).

In order to simulate the upwelling of deeper nutrient-rich seawater to the surface and to promote the development of a phytoplankton bloom, nitrate and phosphate were added to the mesocosms on 2 days (d_0, d_2), to yield concentrations of 10 and 0.65 μmol L^{-1}, respectively. Nutrients were analysed daily and adjusted to ensure equal concentration among mesocosms (Schulz and Riebesell, 2012). Water samples from each mesocosm were collected daily over a period of 21 days by means of a depth-integrating water sampler (HYDROBIOS). The sampler is equipped with a motor and continuously collects a volume of 5 L while being lowered from surface to 9.5 m depth.

In one of the mesocosms (M1), a hole was observed in the TPU foil later during the study. Data from M1 were therefore not considered for analyses.

The carbonate system

The carbonate system was calculated (integrated over the upper 9.5 m) from measured temperature, salinity, pH and total alkalinity (TA) using the stoichiometric stability constants for carbonic acid from Mehrbach *et al.* (Mehrbach *et al.*, 1973) as refitted by Lueker *et al.* (Lueker *et al.*, 2000). Temperature, conductivity, pressure and pH were measured with a CTD (CTD 60 M, Sea and Sun Technology) using a memory probe equipped with an ADM 7-pole conductivity cell (accuracy: ~0.02 salinity units; precision: ~0.005 salinity units), a temperature sensor (Sea and Sun Technology PT100) and a pH sensor (AMT pressure balanced glass electrode together with an Ag/AgCl reference electrode in a plastic housing) with a response time of ~1 s (precision: 0.003 pH units). Practical salinity was calculated from measured conductivity, temperature and pressure according to the UNESCO PSS-78 formulation proposed by Lewis (Lewis, 1980). The measured pH was corrected for offsets with calculated pH (on the total scale) from measured TA and DIC determined coulometrically on sampling time-points t2 and t13. For further details, see Schulz and Riebesell (Schulz and Riebesell, 2012).

Nutrients

Nitrate, nitrite, ammonia, phosphate and silicate were determined from water samples following the methods described by Hansen and Koroleff (Hansen and Koroleff, 1999) within 2 h after sampling by means of an auto-analyser (AA II).

Chlorophyll *a*

The concentration of chlorophyll *a* (Chl *a*) was determined from 250 mL seawater filtered onto glass fibre filters (Whatman GF/F) under low vacuum (<200 mbar), and stored at −20°C before analysis. Pigments were extracted into 10 mL of 90% acetone. Filters were kept overnight in the dark at −20°C and were centrifuged for 10 min at 5000 rpm at 4°C prior to measurement. Chl *a* concentration was determined fluorometrically (TURNER, 10-AU), together with total phaeophytin concentration after acidification (0.1N HCl), according to Welschmeyer (Welschmeyer, 1994). A standard solution of pure Chl *a* was used for calibration.

Organic particles

Samples (400–500 mL) for particulate organic carbon and nitrogen (POC, PON) were filtered (<200 mbar) onto pre-combusted (450°C for 5 h) GF/F filters, and immediately stored frozen at −20°C. Prior to analysis, filters were dried at 60°C and subsequently measured on a EuroVector elemental analyser according to Sharp (Sharp, 1974). Particulate organic phosphorus (POP) was oxidized to orthophosphate with Oxisolv (Merck) in a pressure cooker and determined colorimetrically on a HITACHI V2000 spectrophotometer after Hansen and Koroleff (Hansen and Koroleff, 1999).

Transparent exopolymer particles (TEP)

TEP were detected by staining with Alcian Blue, a cationic copper phthalocyanine dye that complexes carboxyl

(−COO−) and half-ester sulphate (OSO3−) reactive groups of acidic polysaccharides. The amount of Alcian Blue adsorption per sample volume is a measure for TEP concentration and was determined colorimetrically according to Passow and Alldredge (Passow and Alldredge, 1995a,b) from 50 to 100 mL samples, filtered gently (<200 mbar) onto 0.4 μm Nuclepore filters. All filters were prepared in duplicates. The carbon content of TEP was determined after Engel and Passow (Engel and Passow, 2001), applying a (weight:weight) conversion factor of $\Delta TEP:\Delta C = 0.63$.

Bacterial abundance

One millilitre of seawater was vacuum filtered onto black 0.2 μm pore size Nuclepore membranes. The filters were stained with DAPI (4′6′diamidino-2-phenolindole) and stored frozen at −20°C until counting. Filters were counter-stained with 0.1% acridine orange (0.1% W/V, pH 7.2 phosphate buffer) to reduce the background fluorescence of particulate organic and inorganic matter. Bacteria were counted by epifluorescence microscopy (Axio Imager Z1, Zeiss, Germany) at ×1000 magnification.

Activities of microbial extracellular enzymes

The hydrolytic activity potential of the polysaccharide-degrading extracellular enzyme β-glucosidase (βGlcase) and of the protein-degrading leucine-aminopeptidase (LAP) was determined by the use of fluorogenic substrate analogues (Hoppe, 1983). 4-Methyl-umbelliferyl-β-D-glucopyranosid and L-leucyl-4-methylcoumarinyl-7-amide, respectively, were added to 200 μL of sample at final concentrations of 1, 5, 10, 50, 100 and 250 μmol L^{-1}. Fluorescence was measured with a plate reader (FLUOstar OPTIMA, BMG Labtech) immediately after addition of the substrate analogues, and after 3 h of dark incubation close to *in situ* temperature. Wavelengths of 355 and 460 nm were chosen for excitation and the measurement of fluorescence emission, respectively. Calibration of relative fluorescence units was carried out with methylumbelliferone and 7-amino-4-methyl-coumarine standard solutions. V_{max} was derived from the Michaelis−Menten kinetics using SigmaPlot 9.0. Analysis of three replicates revealed a mean standard deviation of about 10%.

DOC and DON

Samples for DOC and for dissolved nitrogen (DN) were collected in combusted glass ampoules after filtration through combusted GF/F filters (24 h 500°C). Samples were acidified with 100 μL of 85% phosphoric acid and stored at 4°C in the dark until analysis. DOC samples were analysed using the high-temperature combustion method (TOC−VCSH, Shimadzu) (Qian and Mopper, 1996). A multi-point calibration curve was established for each day of measurement using potassium hydrogen phthalate standard, which was prepared with MilliQ water. Additionally, two reference seawater standards (Hansell laboratory RSMAS University of Miami) were used to determine the instrument blank. Simultaneously with the DOC measurement, DN compounds were determined by the TNM-1 detector. Therefore, DN is combusted and converted to NOx, which when mixed with ozone gives a chemiluminescence to be detected by a photomultiplier (Dickson *et al.*, 2007). DON was calculated from DN by subtraction of NO_3, NO_2 and NH_4.

Dissolved combined carbohydrates

High-molecular-weight (>1 kDa) dissolved combined carbohydrates (HMW-DCCHO, termed 'dissolved polysaccharides' hereafter) were determined from two replicate samples, filtered through 0.45 μm syringe filters (GHP membrane, Acrodisk, Pall) into precombusted glass vials (24 h at 500°C) using 20 mL disposable syringes. All samples were immediately frozen and stored at −20°C. Prior to filtration, all syringes and syringe filters were rinsed with several millilitres of Milli-Q water first and seawater sample thereafter. The samples were thawed immediately before analytical processing. Carbohydrates were determined by ion chromatography on a Dionex ICS 3000 system using high-performance anion exchange chromatography coupled with pulsed amperometric detection after Engel and Händel (Engel and Händel, 2011). Column temperature was kept constant at 17°C during all analyses. All samples were analysed in duplicate, whereas the standard solutions for calibration were measured in triplicate. Milli-Q water was used as blank to account for potential contamination during sample handling. Blanks were treated and analysed in the same way as the samples and subtracted from sample concentration. Recovery of CCHO was checked by analysing standard solution after every second sample. The detection limit for this method was 10 nmol L^{-1} with a standard deviation between replicate runs of <2%, indicating high precision. Concentrations of dissolved polysaccharides after hydrolysis are given as monomer equivalents. Carbon and nitrogen concentrations of dissolved polysaccharides were calculated based on the chemical formula of identified monomers.

Dissolved free and combined amino acids

Dissolved free amino acids (DFAA) and dissolved combined amino acids (DCAA) were determined by HPLC

after ortho-phthaldialdehyde derivatization (Lindroth and Mopper, 1979). Therefore, 20-mL samples were filtered through 0.45 μm syringe filters with low protein binding affinity (GHP membrane, Acrodisk, Pall Corporation) and stored at −20°C. Samples were thawed immediately before analysis. DCAA were hydrolysed with 6 N HCl at 155°C for 1 h before analysis. Concentrations of DCAA after hydrolysis are given as monomer equivalents. Carbon and nitrogen concentrations of dissolved amino acids (DAA) were calculated based on the chemical formula of identified monomers.

Enrichment experiment

A bottle enrichment experiment was conducted to test for limiting factors in bacterial nutrition. For this purpose, a surface sample collected at the mesocosm site during the initial days of the experiment was filtered through a GF/F filter (~0.8 μm) to exclude grazers. A total of 12 sterile glass bottles (50 mL) were filled with 20 mL filtrate each, containing the free-living fraction of bacterioplankton. Triplicate bottles were amended with either 11.5 μM ammonium (final concentrations), with 12.6 μM glucose (final concentrations), or with a combination of both. Three bottles were left without nutrient addition and served as a control. Cells were incubated for 3 days at *in-situ* temperature and in the dark. Incubations were analysed for bacterial abundances by flow cytometry after nucleic acid staining with Sybr Green I (Invitrogen). For determination of LAP activities, L-leucyl-4-methylcoumarinyl-7-amide was added to final concentrations of 50 μmol L^{-1}. According to the concentration kinetics of LAP in the mesocosms, it must be assumed that 50 μmol L^{-1} of L-leucyl-4-methylcoumarinyl-7-amide represents a non-saturating substrate concentration.

Data analysis

Differences in data, or impact of fCO_2, as revealed by regression analysis were accepted as significant for $P < 0.05$. Average values for total concentrations are given by their arithmetic mean, averages for ratios by their geometric mean. For direct comparison of the different experiments, we defined cardinal time points and spans of the bloom development, such as the bloom peak period, being the days where highest concentrations of Chl *a* were observed (days 4–6), and the bloom sedimentation phase being the phase after the bloom peak during which total nitrogen (TN) concentrations continuously declined within the water column of the mesocosms (Fig. 4). Since the water within the mesocosms was fully oxygenated, such a decline in TN can only be explained by particle sedimentation. Bloom peak concentrations are the arithmetic mean of data from days 4 to 6. Loss of

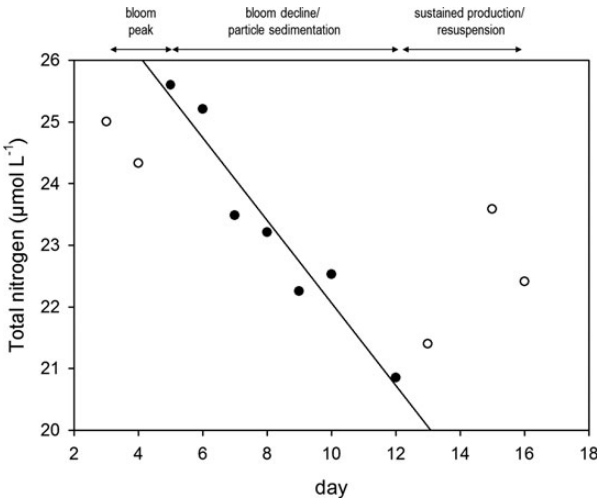

Fig. 4. Temporal development of average concentration of TN, including total dissolved and particulate nitrogen, in the mesocosms, indicating three phases of biogeochemical dynamics, i.e. bloom peak, particle sedimentation after the bloom peak and dissolution/ resuspension of TN towards the study end. Regression line through solid symbols indicate significant decline of TN concentration during days 5–12 ($r^2 = 0.93$, $n = 7$).

POM was calculated as $[\Delta POM] = [POM_{max}] - [POM_{min}]$, with POM_{max} being the maximum concentration observed in each mesocosm during the bloom peak phase, and POM_{min} being the minimum concentration observed in each mesocosm directly after the decline phase. Maximum accumulation of a component was calculated by subtracting the initial (day 3) from the maximum value. Calculations, statistical tests and illustration of the data were performed with Microsoft Office Excel 2010 and Sigma Plot 12.0 (Systat).

RESULTS

Carbonate chemistry perturbation

TA of seawater in the mesocosms ranged between 1911 and 1932 μmol kg^{-1}, and was, as typical for brackish waters, lower than open ocean TA (range: 2270–2350 μmol kg^{-1}; Sarmiento and Gruber, 2006). Addition and utilization of nitrate during the experiment altered TA by about 10 μmol kg^{-1}. The effect on carbonate chemistry, however, was small compared with biological draw down of DIC during the experiment (Schulz and Riebesell, 2012). CO_2 enrichment of the mesocosms was conducted stepwise and finalized after sampling on day 2, yielding a gradient of fCO_2 values on day 3: 355 μatm (M2), 482 μatm (M5), 626 μatm (M3), 760 μatm (M4) and 862 μatm (M6) (Fig. 5a). In the following, we will refer to fCO_2 values determined at day 3 as initial conditions. Addition of high CO_2 seawater to the mesocosms resulted in a decrease of pH.

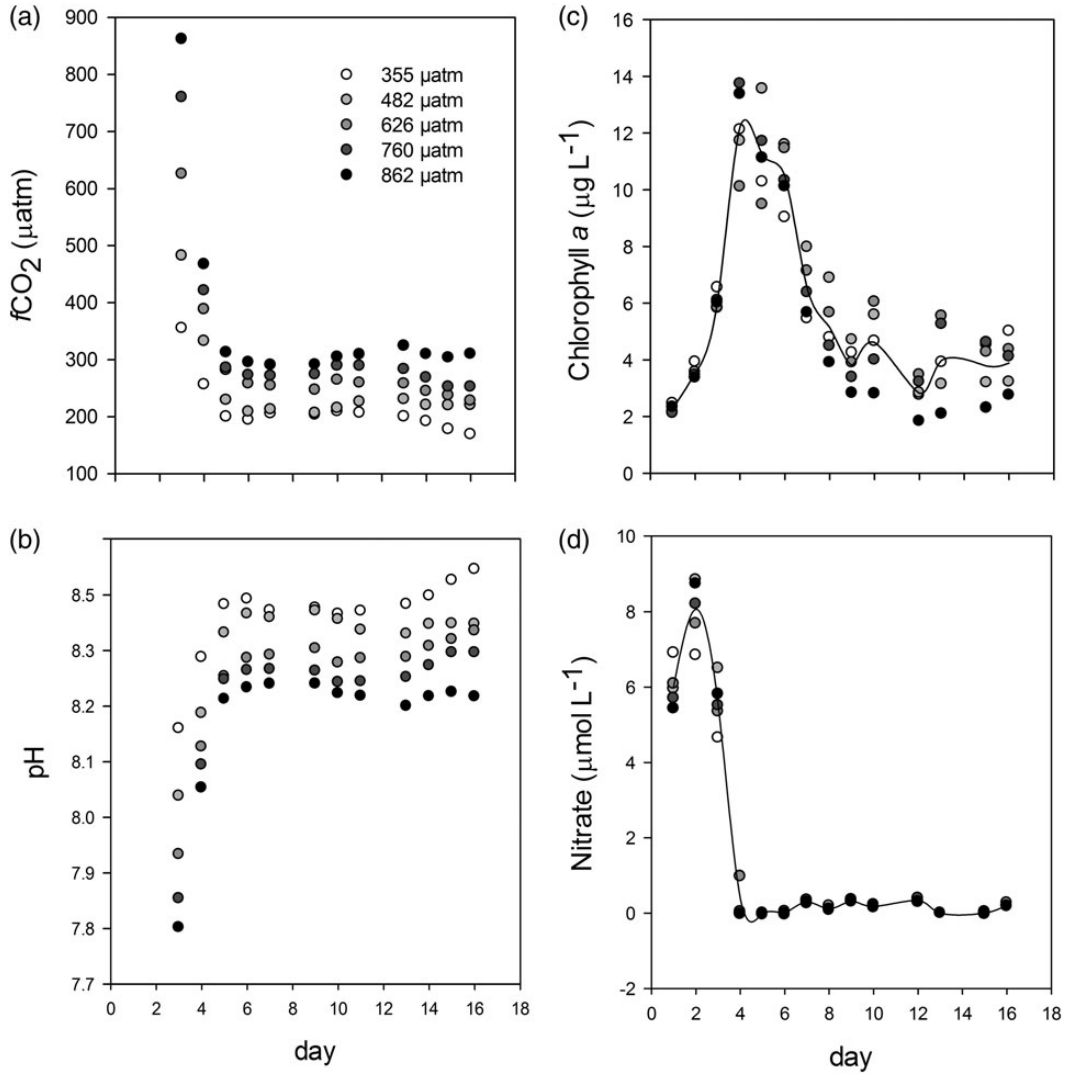

Fig. 5. Development of core parameters in five CO_2-perturbed mesocosms during the phytoplankton bloom experiment. (**a**) fCO_2 (no data available on day 8). (**b**) pH (no data available on day 8). (**c**) Nitrate concentration. (**d**) Chl *a* (no data available on day 11). Symbols of different mesocosms as indicated for initial fCO_2 (µatm), spline curve based on all data.

Values on day 3 ranged from pH (on the total scale) of 7.80 (M6) to 8.17 (M2) (Fig. 5b), with the higher value being comparable with the surrounding water in Kiel Bight (pH 8.16). On day 6, due to photosynthetic uptake of inorganic carbon during the bloom development, fCO_2 and pH had changed strongly in all mesocosms, with fCO_2 varying from 194 to 296 µatm, and pH from 8.39 to 8.23. Thus, carbonate chemistry after the bloom was more similar in all treatments, yet significantly different between the mesocosms ($P < 0.05$).

Bloom development

Nitrate and phosphate were added for a total of 10 and 0.65 µmol L^{-1}, respectively. Silicate concentration was 8 µmol L^{-1} without addition. Nitrite and ammonia were below 0.1 and 0.05 µmol L^{-1}, respectively. Addition of nutrients was conducted on days 0 and 2, and monitored daily by nutrient analyses. Nutrient dynamics and Chl *a* concentration showed typical bloom patterns in all mesocosms. Nutrient concentrations declined rapidly until day 4 (Fig. 5c), concomitant with the increase in Chl *a* concentration. The bloom peak with values of 12 ± 1.7 µg Chl *a* L^{-1} was reached between days 4 and 6 (Fig. 5d). Highest Chl *a* concentrations were observed in the highest fCO_2 treatments (760, 862 µatm), albeit a significant relationship between Chl *a* and fCO_2 was not observed ($P > 0.05$). Chl *a* concentrations strongly declined after the bloom peak and until day 12, suggesting phytoplankton sedimentation, as was also indicated

by loss of TN from the water column (Fig. 4). After day 12, Chl *a* remained relatively stable until the end of the experiment, on day 16. The phytoplankton community inside the mesocosms included cryptophytes (primarily *Teleaulax* sp. and *Plagioselmis* sp.) with highest numbers of 4500 cells mL^{-1} on days 4–5, and diatoms like *Guinardia delicatula* with highest numbers of 900 cells mL^{-1} on day 6. Other, less abundant, phytoplankton species were the diatom *Thalassionema nitzschioides* and dinoflagellates (primarily *Gymnodiniales*).

Particulate organic matter dynamics

POM concentrations followed the phytoplankton bloom development. Starting from initial values of 28 ± 0.7, 3.8 ± 0.2 and 0.2 ± 0.01 μmol L^{-1} for POC, PON and POP, respectively, POM increased in all mesocosms until the peak of the bloom on days 4–6 (Fig. 6a–c). C, N and P in particulate matter were closely coupled to each other during the biomass build-up phase, and exhibited higher carbon and nitrogen assimilation relative to phosphorus when compared with Redfield stoichiometry of 106:16:1 (Table I). Values of Δ[POC]:Δ[PON] were significant positively related to initial fCO_2 ($P < 0.05$), whereas no impact of fCO_2 was identified for Δ[PON]:Δ[POP] or Δ[POC]:Δ[POP]. After the bloom peak, POM declined in all mesocosms due to particle sedimentation. The loss of POM during the decline phase (days 5–12) was most pronounced for PON and POP, while POC remained at a relatively high level. During the last days of the study (days 13–16), PON and POP, but not Chl *a* increased again slightly. Thus, at the height of the bloom (days 4–6),

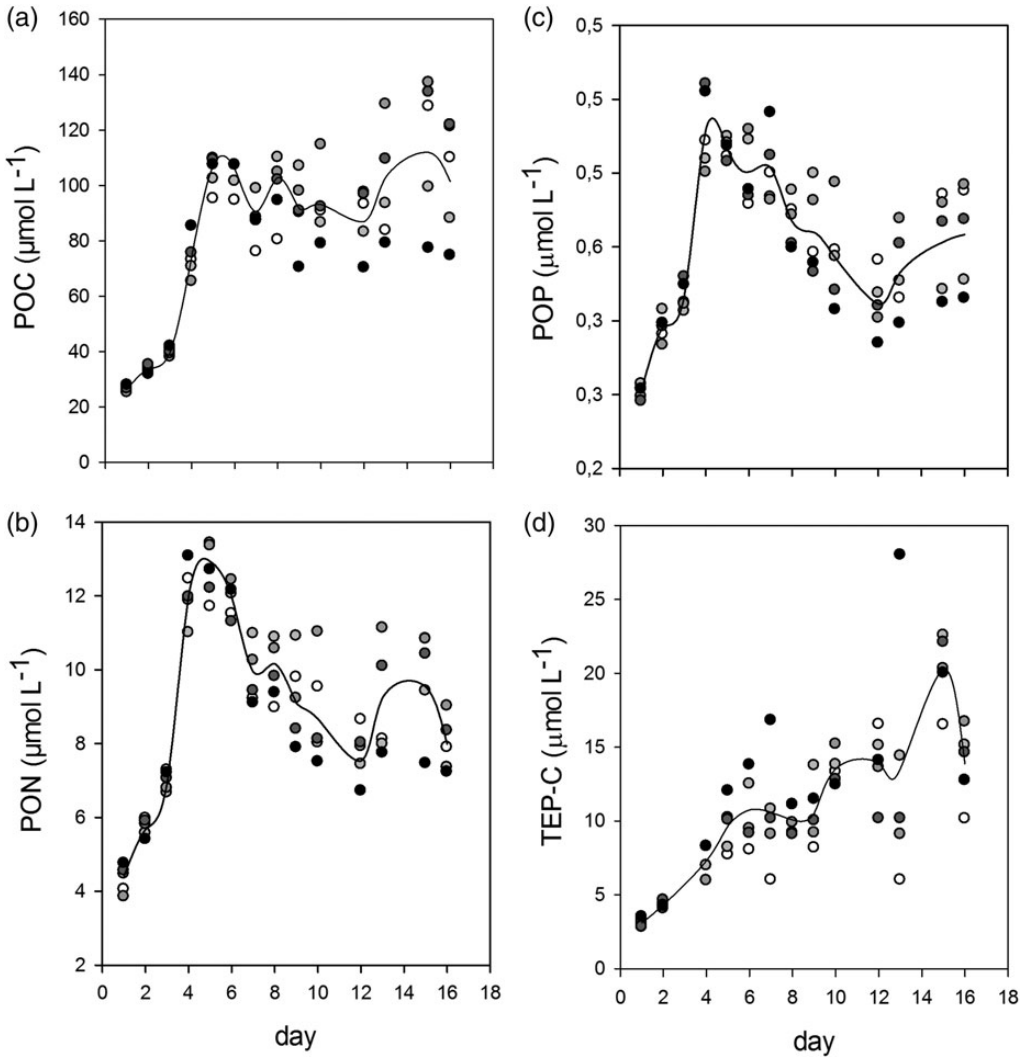

Fig. 6. (**a**–**f**) Development of particulate organic components during the phytoplankton bloom experiment in 5 CO_2-perturbed mesocosms. (a) POC, (b) PON, (c) POP, (d) TEP. Symbols and lines as in Fig. 5.

Table I: Changes in element stoichiometry of organic particles during the rise of the bloom (days 0–6) as determined by the slope (a) of the linear regression.

	Initial fCO_2 (μatm)										
	355		482		626		760		862		
	a	r^2	*a*	r^2	*a*	r^2	*a*	r^2	*a*	r^2	$<P$
ΔPOC:ΔPON	7.8	0.93	8.4	0.98	8.3	0.94	9.3	0.93	8.8	0.96	0.05
ΔPON:ΔPOP	24.5	0.99	23.8	0.98	25.1	0.99	21.2	0.95	22.9	0.97	n.s.
ΔPOC:ΔPOP	188	0.90	198	0.95	209	0.94	179	0.78	189	0.87	n.s.

Initial fCO_2 was obtained on day 3; *P*: significance level for correlation between slope values and initial fCO_2.

Table II: Contribution of different components to carbon and nitrogen pools

		Initial fCO_2 (μatm)									
		355		482		626		760		862	
		Avg.	SD	Avg.	SD	Avg.	SD	Avg.	SD	Avg.	SD
DCCHO	μmol C L^{-1}	24	7.6	23	7.9	25	7.0	25	6.6	24	7.1
DFAA	μmol C L^{-1}	0.2	0.11	0.17	0.07	0.2	0.07	0.17	0.04	0.20	0.12
DCAA	μmol C L^{-1}	16	5.0	15	6.0	16	6.6	14	7.4	15	8.4
DFAA	μmol N L^{-1}	0.05	0.035	0.05	0.02	0.05	0.02	0.05	0.02	0.06	0.04
DCAA	μmol N L^{-1}	4.9	1.4	4.6	1.8	5.0	1.9	4.3	2.2	4.7	2.6
DOC*	% DOC	14	2.5	13	2.0	14	2.5	13	2.5	15	1.4
DON*	%DON	34	17	35	9	42	11	41	11	45	8
DOC*:DON*	(mol:mol)	9.3	2.3	8.3	1.8	8.8	2.0	8.3	1.8	7.2	0.7
DOC:DON	(mol:mol)	24	2.0	23	2.6	23	1.2	23	2.7	23	2.2
TEP-C	μmol C L^{-1}	9	4.8	12	4.9	10	5.0	10	4.8	13	19
TEP-C	(% POC)	10	0.03	13	0.04	11	0.02	11	0.02	16	0.07

Avg.: averaged values over the study period (days 3–16), SD: standard deviation. Values for fCO_2 as determined on day 3 of the experiment. DOC* and DON*: chemically characterized components of DOM.

POM exhibited a lower PON:Chl *a* ratio of 0.94 ± 0.34, compared with the post-bloom phase (days 12–16) with a PON:Chl *a* ratio of 2.2 ± 0.48. This suggests a greater partitioning of nitrogen into autotrophic plankton during the bloom, shifting towards a more detrital or heterotrophic community later during the study.

Coagulation and spontaneous assembly of macromolecules like polysaccharides leads to the formation of nanogels and subsequently of gel particles known as TEP. During this study, TEP concentrations inside the mesocosms increased continuously from an initial average of 3.6 ± 0.34 μmol C L^{-1} to reach highest values of 16 μmol C L^{-1} in the low fCO_2 treatment (355 μatm) on day 15, and 28 μmol C L^{-1} in the high fCO_2 treatment (862 μatm) on day 13 (Fig. 6d). The continued increase in carbohydrate-rich TEP (Fig. 6d) partly compensated for the loss of POC due to plankton sedimentation and can explain why POC concentrations remained at a relatively high level during days 5–12, compared with PON and POP. TEP-C was equivalent to 10–16% of POC, with the highest ratio observed in the highest fCO_2 mesocosm (Table II). Although a direct influence of fCO_2 on TEP concentration during the study was not revealed for the entire period, accumulation of TEP during the bloom peak period (TEP_{peak}) calculated as the average of days 4–6 was significantly related to average fCO_2 during this period ($P = 0.01$) (Fig. 7a). Moreover, maximum TEP concentration, observed later during the study (days 13–15), also correlated significantly with average fCO_2 ($P < 0.05$). TEP enhance total particle abundance as well as bulk particle stickiness and play a significant role in the formation and sinking of aggregates. During this study, significant direct relationships were observed between TEP_{peak} concentrations and the loss of POC as well as of POP during the period of bloom sedimentation (days 5–12) (Fig. 7b and d). The loss of PON also increased with increasing TEP_{peak} concentration, but this pattern was less significant ($P = 0.06$) (Fig. 7c). No significant relationship was observed between the concentrations of POC, PON and POP at the bloom peak and the loss of these components during the decline phase, suggesting that sedimentation was not a direct function of POM abundance.

Variability of concentrations of POM components, i.e. Chl *a*, POC, PON, POP, and TEP among the mesocosms, clearly increased after the bloom peak. Initial

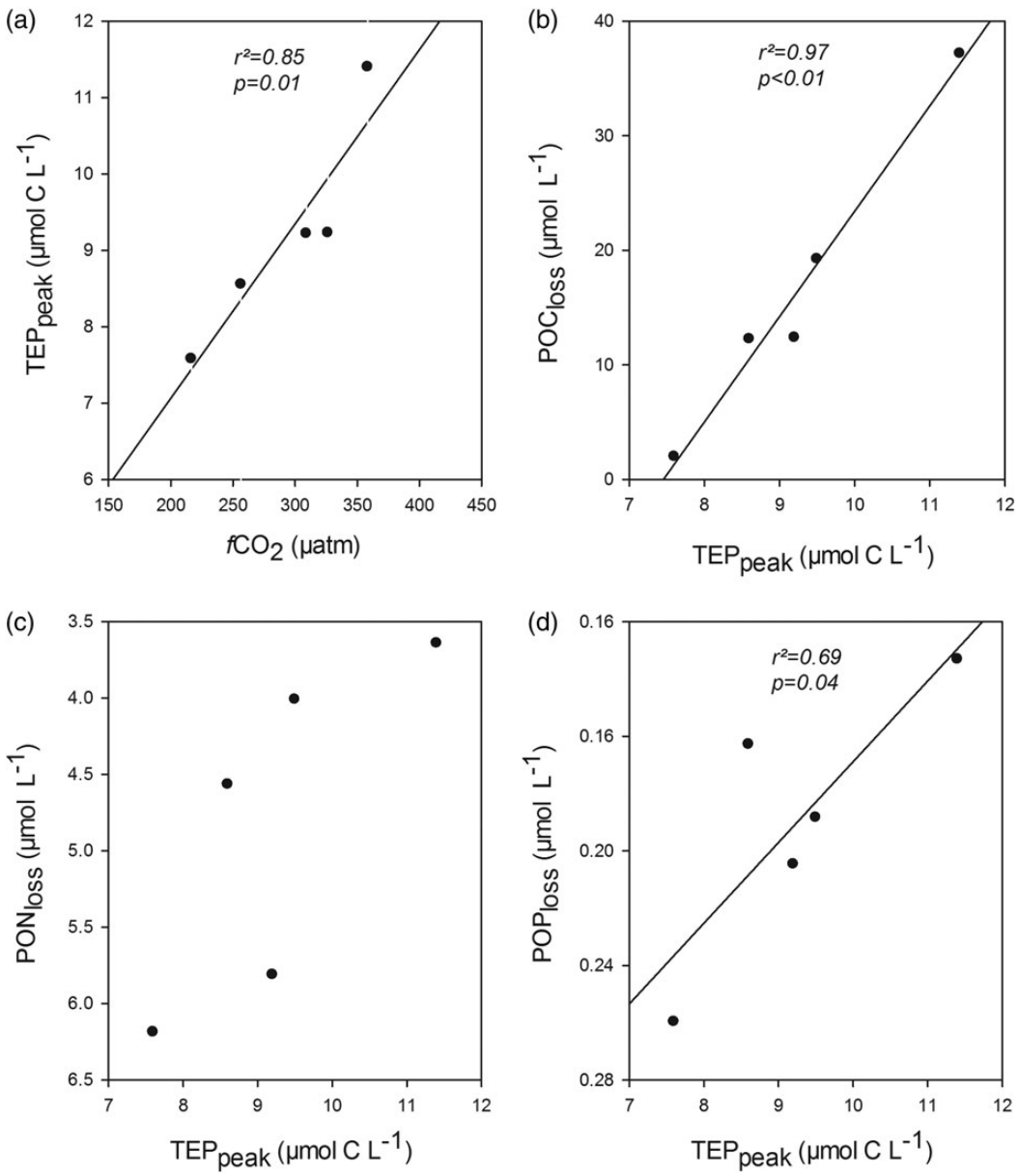

Fig. 7. Relationship between average fCO_2 and TEP concentration (TEP_{peak}) at the time of the bloom peak (days 4–6) (**a**), as well as the relationships between TEP_{peak} and the loss of particulate organic carbon (POC, **b**), nitrogen (PON, **c**) and phosphorus (POP, **d**) after the bloom peak (days 5–12).

variability calculated as standard deviation divided by the mean value was <5% for all components and increased to about 20% by the end of the study.

Dissolved organic matter dynamics

DOM clearly differed from POM dynamics in all mesocosms. Initial DOC concentrations were 281 ± 12 µmol L^{-1}, and increased continuously until day 12 in all mesocosms (Fig. 8a). DOC concentrations in the Baltic Sea are relatively high (range: 270–600 µmol L^{-1}), and reflect both the terrestrial run-off and the high refractory load (Kulinski and Pempkowiak, 2008). Maximum accumulation of fresh DOC in each mesocosm, calculated as $[DOC_{max}] - [DOC_{initial}]$, ranged between 42 and 78 µmol L^{-1}, and was not related to fCO_2 ($P = 0.44$). A decrease in DOC was observed towards the end of the study, particularly in the mesocosm with highest fCO_2 (862 µatm). DON concentrations started with an average of 12 ± 0.72 µmol L^{-1}, varied strongly during the first 4 days and ranged between 12 and 16.6 µmol L^{-1} thereafter (Fig. 8b). Thus, bloom development did not result in

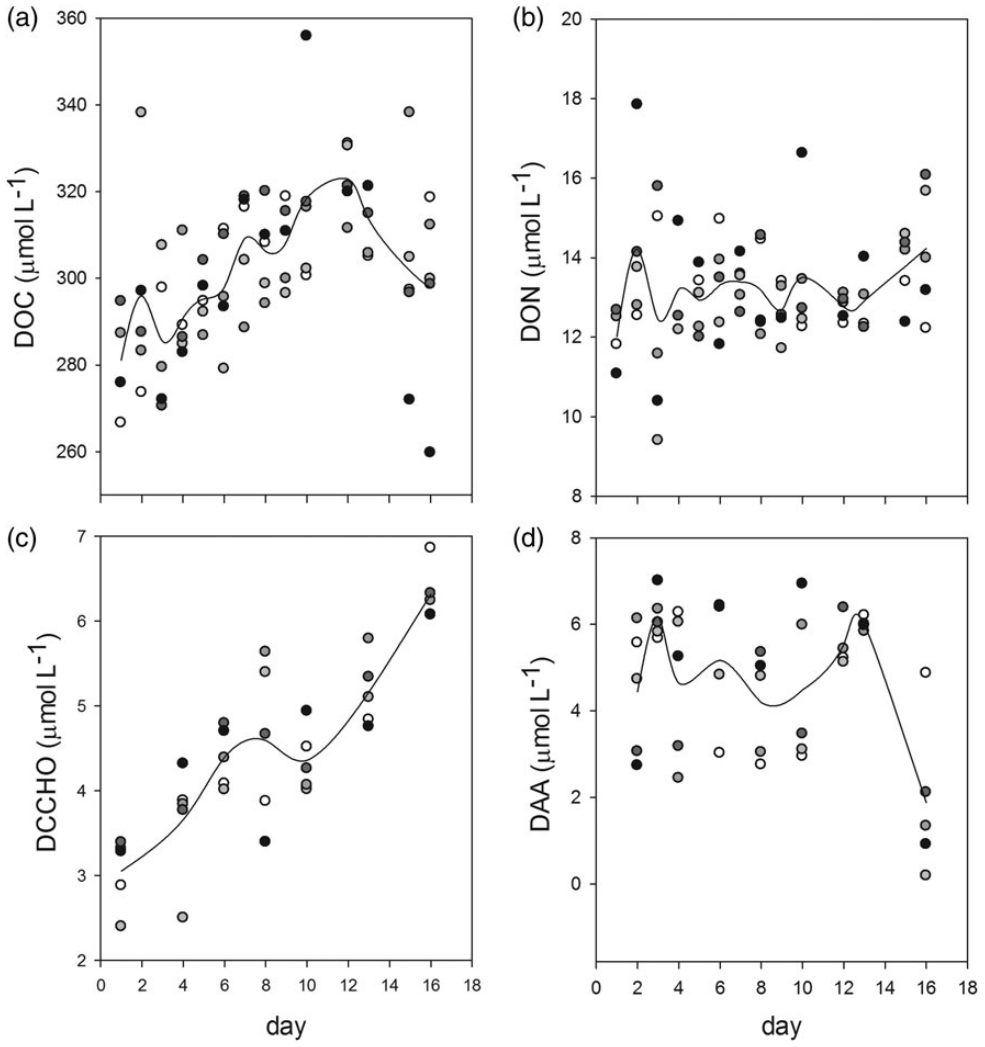

Fig. 8. Development of dissolved organic components during the phytoplankton bloom in CO_2 perturbed mesocosms. (**a**) DOC, (**b**) DON, (**c**) dissolved polysaccharides (HMW-DCCHO), (d) DAA, including dissolved free and combined amino acids. Symbols and lines as in Fig. 4.

a net accumulation of DON over the observation period. DON concentrations in the mesocosms were not related to CO_2 addition ($P = 0.67$).

DOC and DON concentration ratios (mol:mol, geometric mean) averaged over the whole period ranged between 23 and 24 in the different mesocosms (Table II), and were not significantly related to the CO_2 treatment. In the course of the bloom, i.e. between days 4 and 12, [DOC]:[DON] ratios increased in all mesocosms from 21 to 26, therewith showing a selective enrichment of carbon-rich substances compared with the Redfield ratio of 6.625.

Two fractions of DOM, DAA and HMW-DCCHO, i.e. mainly polysaccharides, were determined during this study and displayed different temporal developments. Polysaccharide concentration yielded an average of 2.5 ± 0.36 µmol L^{-1} initially, and accumulated continuously in the course of the experiment in all mesocosms (Fig. 8c). Accumulation of fresh polysaccharides over the study period ranged between 3.3 (760 µatm) and 4.2 (350 µatm) µmol L^{-1}, corresponding to 15–23 µmol L^{-1} fresh DOC. No direct effect of fCO_2 on polysaccharide concentration was observed ($P = 0.12$).

In contrast to polysaccharides, we observed no accumulation of DAA, including DFAA and DCAA (Fig. 8d). DAA concentrations varied between 2.4 and 7.0 µmol L^{-1} until day 16, when DAA concentrations markedly declined. Concentrations of DFAA were low throughout the study period and ranged between 16 and 127 nmol L^{-1}, comprising on average $1.9 \pm 4.2\%$ of DAA. No significant effect of fCO_2 was observed on DCAA or DFAA concentrations either ($P = 0.7$).

Dissolved polysaccharides and DAA comprise the majority of freshly produced DOC during phytoplankton

blooms (Engel *et al.*, 2011). In order to estimate the amount of fresh and potentially bioavailable DOM accumulation during this mesocosm experiment, carbon and nitrogen concentrations of dissolved polysaccharides and DAA were calculated based on chemical formulas of monomers determined. In this way, identified DOC and DON are referred to as DOC* and DON* hereafter (Table II). DOC* ranged between 9 and 18% of DOC, and DON* between 34 and 45% of DON. Hence, the fraction of uncharacterized DOC was much larger than the fraction of uncharacterized DON. Ratios of [DOC*]:[DON*] were lower than bulk [DOC]:[DON] ratios and ranged between 7.2 and 9.3. Thus, the C:N ratio of identified and potentially bioavailable DOM was more similar to Redfield stoichiometry than in bulk DOM.

In contrast to POM, variability of dissolved components did not change markedly over time.

Bacteria and hydrolytic enzymes

Initial abundance of bacteria inside the mesocosms was $1.15 \times 10^6 \pm 1.65 \times 10^5$ cells mL^{-1} on average. Abundances of bacteria (Fig. 9a) increased in the wake of the bloom, ranging from maximum values of 1.2×10^6 cells mL^{-1} in the two mesocosm with lowest fCO_2 (355, 482 μatm) to 1.6×10^6 cells mL^{-1} in the mesocosm with highest fCO_2 (862 μatm). Maximum abundances of bacteria were observed during the post-bloom phase and were strongly related to initial fCO_2 (Fig. 9b, $P < 0.01$). An abrupt decline of bacterial abundance occurred during the last 2 days of the study, coinciding with high TEP abundance. This can be explained by a higher fraction of particle attached bacteria potentially underestimated during microscopic counting.

The organic matter degradation potential of bacteria was assessed from activities (V_{max}) of the hydrolytic extracellular enzymes βGlcase and LAP, respectively (Fig. 10a and b). LAP activity started to increase immediately after the Chl *a* peak on day 9 and declined before the end of the experiment. Activity of βGlcase rose from days 11 to 12 on and did not culminate until the end of the experiment in most mesocosms. Highest rates for βGlcase and LAP were 54–88 and 8.2–11.5 μmol L^{-1} day^{-1}, respectively. Enzyme activities were not significantly related to the CO_2 treatment.

The response of free-living bacteria to nutrient enrichment was tested during the first days of the study. The initial abundance of free-living bacteria was 2.0×10^5 cells mL^{-1}, representing about 20% of the total bacterioplankton community. After 3 days of incubation, cell numbers in ammonium amended samples were significantly higher than in samples without ammonium (*t*-test, $P = 0.03$), suggesting nitrogen limitation of bacterial growth (Fig. 11a). Concomitantly, cell-specific rates of LAP in samples with ammonium supply were significantly lower than in incubations without nitrogen enrichment (*t*-test, $P = 0.02$) (Fig. 11b). Reduced LAP activity revealed a reduced potential for the hydrolysis of proteins in ammonium-enriched samples, thereby supporting the assumption that enhanced growth was largely based on the utilization of inorganic nitrogen.

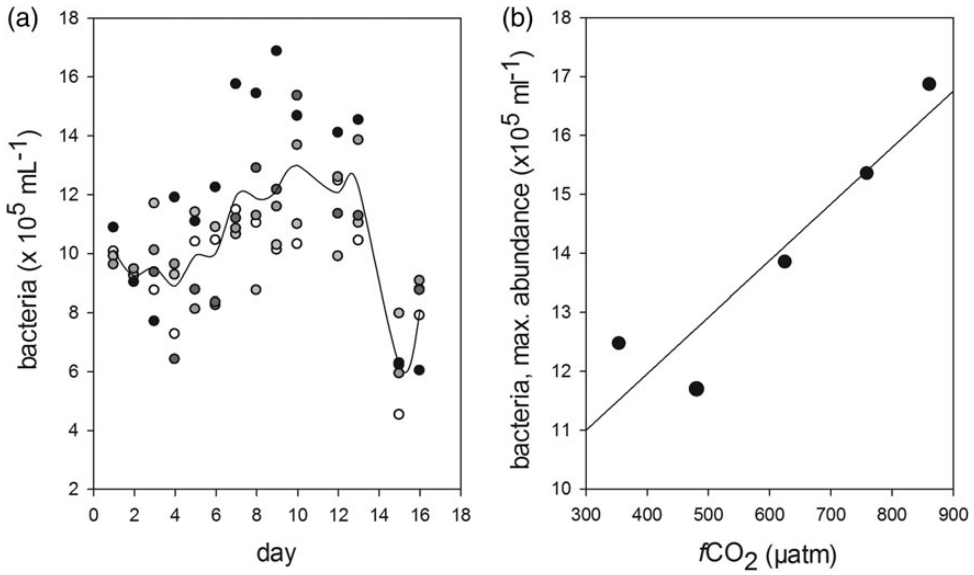

Fig. 9. (**a**, **b**) Abundance of heterotrophic bacteria during the bloom development in five CO_2 perturbed mesocosms (a), and the relationship between maximum bacterial abundance determined per mesocosms and its initial fCO_2.

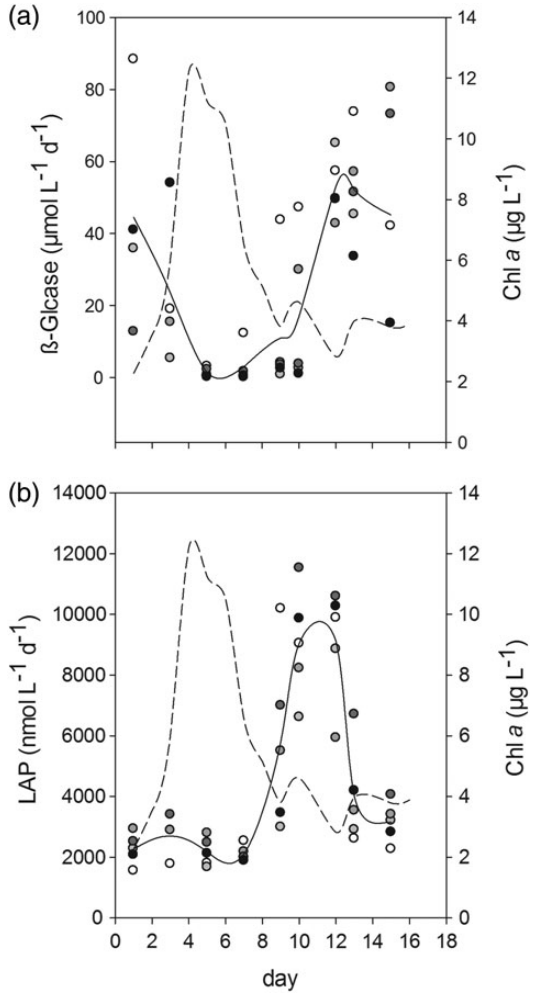

Fig. 10. (**a**, **b**) Development of the maximal activity (Vmax) of the extracellular enzymes leucine-aminopeptidase (LAP) and βGlcase in the course of the phytoplankton bloom, as indicated by Chl *a* concentration. Symbols and lines as in Fig. 4.

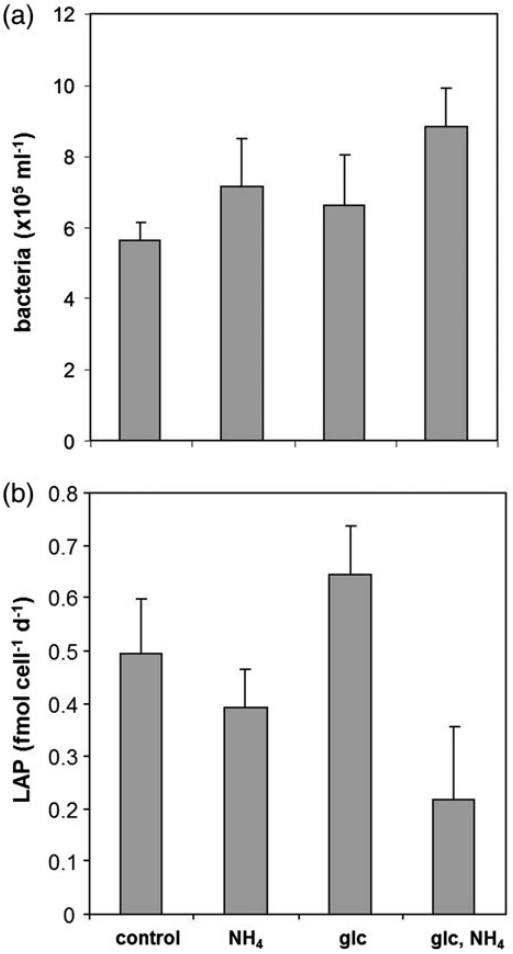

Fig. 11. Response of bacterioplankton abundance (**a**) and of cell-normalized LAP activities (**b**) to the amendment of ammonium (N) and glucose (glc) as inorganic nitrogen and labile carbon sources.

DISCUSSION

CO_2 effects on POM dynamics

This mesocosm study was conducted to study effects of CO_2 enrichment on organic matter dynamics during coastal phytoplankton blooms. Addition of nutrients to the mesocosms directly initiated bloom development, in the wake of which pH and fCO_2 changed strongly. The temporal development of POM dynamics was rather similar in all mesocosms and exhibited a clear bloom peak with subsequent decline of Chl *a*, and particulate element concentrations. Variability among the mesocosms clearly increased after the bloom peak (days 4–6) for all POM components. One factor known to induce the loss of POM from surface waters during bloom periods is the settling of individual particles as well as of particle aggregates. Particle aggregate formation is a complex, non-linear process and depends on the abundance of particles as well as on their collision rates and surface stickiness. Because all mesocosms were constructed in the same way and deployed close to each other, strong differences between mesocosms with respect to water column physics, such as temperature, turbulence and density, that could affect particle collision rates differentially seem unlikely.

An important factor determining phytoplankton aggregation dynamics is the abundance of TEP. TEP increase bulk particle abundance and stickiness, and hence the rate of initial aggregate formation (Engel, 2000; Mari and Robert, 2008). Thus, at comparable cell abundance, a higher TEP concentration would rise the amount of cells being included in aggregates, likely enhancing particle sedimentation. During this study, we observed a significant relationship between the concentration of TEP at the time of highest phytoplankton abundance, i.e. TEP_{peak}, and the subsequent sedimentation loss of

particles. An increase in TEP abundance has frequently been shown to induce phytoplankton aggregation in earlier mesocosm studies (Passow and Alldredge, 1995a,b; Engel *et al.*, 2005; Kahl *et al.*, 2008), as well as in the field (Passow *et al.*, 2001; Engel, 2002; Mari *et al.*, 2012). Thereby, the transition between a state of mainly suspended particles and another where particles are included in aggregates is supposedly fast during phytoplankton blooms, i.e. <2 days (Jackson, 1990), and could explain rapid loss of POM from the water column observed in the mesocosms. Because TEP include carbohydrates that originate from photosynthetic production, it has been suggested that an enhanced uptake of inorganic carbon under high fCO_2 would also enhance carbohydrate exudation, subsequently favouring TEP production and vertical particle export (Engel, 2002; Arrigo, 2007). Observations supporting this hypothesis, however, are scarce and controversial. Engel (Engel, 2002) and Borchard and Engel (Borchard and Engel, 2012) observed that TEP concentrations increased with increasing pCO_2 in nutrient-limited phytoplankton. Mari (Mari, 2008) suggested that CO_2-induced acidification may also directly increase TEP concentration as lower pH would result in more swollen structures and larger TEP volume. Passow (Passow, 2011), however, tested acidification effects on TEP formation, and concluded that pH does not influence abiotic TEP formation. Similarly, Thornton (Thornton, 2009) observed no direct pH effect on TEP formation, but determined a higher release of low-molecular weight carbohydrates in cultures of the diatom *Chaetoceros muelleri* at low pH. This mesocosm study showed a positive relationship between initial fCO_2 and TEP_{peak} concentration, as well as between TEP_{peak} concentration and POM loss and supports the hypothesis that CO_2-enhanced TEP formation could favour particle aggregate formation and settling during marine phytoplankton blooms. Because TEP are a product of autotrophic production and enriched in organic carbon (Engel and Passow, 2001), higher TEP_{peak} concentrations at higher initial fCO_2 agree well with the observed steeper increase in POC relative to PON concentration during the bloom build-up phase, as well as with a higher biomass normalized utilization of DIC that was also observed during this study (Schulz and Riebesell, 2012).

Another factor potentially responsible for aggregate formation is bacterial abundance (Smith *et al.*, 1992). Bacterial exudates are highly sticky and induce bacterial aggregation as well as TEP formation (Grossart *et al.*, 1997; Simon *et al.*, 2002; Gärdes *et al.*, 2011). Maximal bacteria abundance was significantly related to initial fCO_2 during this study. Because TEP also provide a structural substrate for marine bacteria to attach and grow, cause and effect of TEP and bacteria abundance and their relation to the CO_2 treatment cannot be discriminated unambiguously. However, the cell-specific TEP production of bacterioplankton has been estimated to be 0.1 fg Xeq. $cell^{-1}$ h^{-1} (Stoderegger and Herndl, 1999), which would yield a contribution of 20% at most to the total TEP accumulation over the course of this study. Hence, it seems more likely that at high fCO_2 bacteria benefitted from higher TEP concentration rather than TEP production being increased by higher bacterial abundance.

CO_2 effects on DOM dynamics

The imprint of the phytoplankton bloom was clearly different for DOM compared with POM dynamics, and differed also between carbon and nitrogen components. While DOC and dissolved polysaccharides accumulated over the course of the study, no clear changes were observed for DON or DAA. A temporal decoupling of DOC from DON cycling in the surface ocean, and a deviation of DOC:DON ratios from Redfield stoichiometry have been suggested earlier, specifically for post-bloom systems (Williams, 1995; Kaehler and Koeve, 2001). This has been related to the accumulation of semi-labile DOC due to extracellular release of photosynthetic products (Anderson and Williams, 1998; Schartau *et al.*, 2007) as well as to a reduction in DOC break-down by microorganisms being nutrient limited or top-down controlled by grazing (Thingstad *et al.*, 1997). Moreover, bacteria have a rather low C:N ratio and discriminate against organic carbon, which favours increasing C:N ratios during degradation. Turn-over times for dissolved polysaccharides are typically in the range of several weeks to months (Skoog and Benner, 1997; Kirchman *et al.*, 2001; Piontek *et al.*, 2011) and accumulations of polysaccharides are regularly observed after the spring bloom in coastal seas (Ittekkot *et al.*, 1981; Engel *et al.*, 2012). While carbohydrates are tightly related to algal photosynthesis, the concentration of DAA in seawater is also determined by viral and heterotrophic activity solubilizing particulate matter (Chrost *et al.*, 1998). Fresh DAA are a preferred and valuable nutritious organic resource for heterotrophic microorganisms, and rapidly turned over (hours–days) in aquatic systems (Bronk, 2002). During this study, amino acids explained 30–50% of the DON pool. This is higher than observed for many oceanic surface waters (Benner, 2002), but comparable with previous findings in the Baltic Sea (Engel *et al.*, 2011). Thus, temporal DOM dynamics as observed during this mesocosm bloom experiment are consistent with previous findings for surface ocean and coastal seas.

CO_2 perturbation of the mesocosms did not significantly change concentrations of DOC and DON, or of

the major components polysaccharides and DAA. The absence of a CO_2 effect on dissolved polysaccharide concentration was contrary to our expectation that higher CO_2 concentration favours the extracellular release from phytoplankton. One explanation may be the rapid partitioning of polysaccharides from the dissolved phase into the TEP pool that already increased after the first days of the study and likely counteracted the accumulation of excess exudates in the dissolved fraction.

Rapid microbial turn-over likely prevented the accumulation of labile DAA, and impeded the determination of a CO_2 response, if there was any. However, background concentrations of DCAA were high, indicating the presence of a semi-labile DON pool. Future studies may need to address dynamics of labile and semi-labile DOM with a higher temporal resolution to identify effects of altered fCO_2 or pH.

CO_2 effect on microbial enzyme activities

The response of bacterioplankton to ammonium enrichment in the side experiment revealed the utilization of inorganic nitrogen for growth. Hence, it seems likely that bacteria were strong competitors to phytoplankton for inorganic nutrients supplied to mesocosms during the initial days of the study. For the degradation of organic substrates, a first step is the cleavage of high molecular weight substrates such as dissolved polysaccharides and proteins into smaller subunits by extracellular, mainly bacterial, enzymes (Chrost *et al.*, 1998). Piontek *et al.* (Piontek *et al.*, 2010) showed that the hydrolytic cleavage of polysaccharides increased together with the activity of extracellular glucosidases when seawater became more acidic and suggested that ocean acidification will affect the microbial consumption of DOM. During this study, no significant differences between the CO_2 treatments were determined with respect to the polysaccharide and peptide degrading enzymes βGlcase and LAP, respectively. However, highest activities of both enzymes were observed after day 6 when the bloom had already reduced acidity levels considerably. Thus, a direct effect of acidification on enzyme activities could not be determined at that time.

As revealed by the nitrogen enrichment experiment, bacterioplankton growth and activity were limited by the availability of nitrogen during the initial bloom phase. The temporal development of extracellular enzyme activity moreover suggests that nitrogen limitation of bacterioplankton prevailed also in the post-bloom phase. The high bacterial demand suggests rapid turn-over of labile nitrogen and can explain why no accumulation of DON was observed during bloom development, while DOC concentrations increased. The limitation of bacterial activity by nitrogen likely hampered an effective turnover of labile and semi-labile carbon compounds on the timescale of this experiment, thereby potentially promoting the accumulation of TEP.

Implications for coastal ecosystems

Uptake of atmospheric CO_2 is responsible for a decline of seawater pH in the open ocean, known as ocean acidification. This process is fast compared with seawater fCO_2 induced changes on geological timescales, but may be slow relative to the timescales of physiological acclimation and evolutionary adaptation of many marine microorganisms (Joint *et al.*, 2011). In coastal seas, changes in seawater pH and carbonate chemistry result from a multitude of different processes such as upwelling of CO_2-rich deeper water, nitrate and phosphate eutrophication, or river-discharge, and occur on seasonal or annual timescales. Acidification due to uptake of anthropogenic CO_2 will overlay these processes and may greatly amplify pH variations in coastal seas (Blackford and Gilbert, 2007; Cai *et al.*, 2011). Equilibration with atmospheric CO_2 as well as mixing with CO_2-rich deep water determines seawater carbonate chemistry at the beginning of the spring period in coastal systems. This study has shown that increasing initial fCO_2 can support the rate accumulation of POC, particularly TEP, during bloom development, and lead to a higher abundance of heterotrophic bacteria. Thereby, the higher bacterial abundance is likely an indirect effect and due to the increased structural and nutritional substrate availability of TEP. Because TEP induce aggregate formation, a CO_2-increased TEP concentration at the time of highest particle abundance, i.e. bloom height, may lead to higher settling loss of POM to the seafloor, particularly in the shallow Baltic Sea. Hence, increasing CO_2 concentrations may impact coastal biogeochemistry in a similar way as eutrophication, that is to increase the total amount of organic matter available for planktonic and benthic microbial remineralization. Combined occurrence of acidification and eutrophication could thus amplify the loss of oxygen and enhance the already widespread anoxia of the Baltic Sea subsurface waters during summer months.

ACKNOWLEDGEMENTS

We thank Nicole Händel, Stefan Rösel, Christian Wurzbacher, Jon Roa, Tobias Mattfeld, Michael Meyerhöfer and Peter Fritsche for technical assistance and help during sampling. The Boknis Eck Time Series Station (BE) is operated by the Chemical Oceanography

department at GEOMAR: www.bokniseck.de. Hermann Bange is gratefully acknowledged for providing access to the BE data.

FUNDING

This study was supported by the Helmholtz Association (HZ-NG-102) and by the BMBF projects SOPRAN (03F0611C) and BIOACID (03F0608E). Work of M.S. was supported by the Helmholtz Graduate School for Polar- and Marine Sciences (POLMAR).

REFERENCES

Alldredge, A. L., Passow, U. and Logan, B. E. (1993) The abundance and significance of a class of large. Transparent organic particles in the ocean. *Deep-Sea Res.*, **40**, 1131–1140.

Anderson, T. R. and Williams, P. J. L. (1998) Modelling the seasonal cycle of dissolved organic carbon at station E-1 in the English Channel. *Estuarine Coastal Shelf Sci.*, **46**, 93–109.

Arrigo, K. R. (2007) Carbon cycle. Marine manipulations. *Nature*, **450**, 491–492.

Bellerby, R. G. J., Schulz, K. G., Riebesell, U. *et al.* (2008) Marine ecosystem community carbon and nutrient uptake stoichiometry under varying ocean acidification during the PeECE III experiment. *Biogeosciences*, **5**, 1517–1527.

Benner, R. (2002) Chemical composition and reactivity. In Hansell, D. A. and Carlson, C. (eds), *Biogeochemistry of Marine Dissolved Organic Matter.* Academic Press, Elsevier Science, pp 59–90.

Blackford, J. C. and Gilbert, F. J. (2007) pH variability and CO2 induced acidification in the North Sea. *J. Mar. Syst.*, **64**, 229–241.

Borchard, C. and Engel, A. (2012) Organic matter exudation by *Emiliania huxleyi* under simulated future ocean conditions. *Biogeosciences*, **9**, 3405–3423.

Bronk, D. A. (2002) Dynamics of DON. In Hansell, D. A. and Carlson, C. (eds), *Biogeochemistry of Marine Dissolved Organic Matter.* Academic Press, Elsevier Science, pp 59–90.

Cai, W. J., Hu, X., Huang, W. J. *et al.* (2011) Acidification of subsurface coastal waters enhanced by eutrophication. *Nat. Geosci.*, **4**, 766–770.

Chrost, R. J., Hoppe, H., Grossart, H. P. *et al.* (1998) The significance of limnetic organic aggregates (lake snow) for the sinking flux of particulate organic matter in a large lake. *Aquatic Microb. Ecol.*, **15**, 115–125.

Dickson, A. G., Sabine, C. L. and Christian, J. R. (eds) (2007) *Guide to Best Practices for Ocean CO2 Measurements*. PICES Press, Special Publication 3.

Engel, A. (2000) The role of transparent exopolymer particles (TEP) in the increase in apparent particle stickiness (alpha) during the decline of a diatom bloom. *J. Plankton Res.*, **22**, 485–497.

Engel, A. (2002) Direct relationship between CO_2 uptake and transparent exopolymer particles production in natural phytoplankton. *J. Plankton Res.*, **24**, 49–53.

Engel, A. and Passow, U. (2001) Carbon and nitrogen content of transparent exopolymer particles (TEP) in relation to their Alcian Blue adsorption. *Mar. Ecol. Prog. Ser.*, **219**, 1–10.

Engel, A. and Händel, N. (2011) A novel protocol for determining the concentration and composition of sugars in particulate and in high molecular weight dissolved organic matter (HMW-DOM) in seawater. *Mar. Chem.*, **127**, 180–191.

Engel, A., Händel, N., Wohlers, J. *et al.* (2011) Effects of sea surface warming on the production and composition of dissolved organic matter during phytoplankton blooms: results from a mesocosm study. *J. Plankton Res.*, **33**, 357–372.

Engel, A., Harlay, J., Piontek, J. *et al.* (2012) Contribution of combined carbohydrates to dissolved and particulate organic carbon after the spring bloom in the northern Bay of Biscay (North-Eastern Atlantic Ocean). *Cont. Shelf Res.*, **45**, 42–53.

Engel, A., Zondervan, I., Aerts, K. *et al.* (2005) Testing the direct effect of CO2 concentration on a bloom of the coccolithophorid *Emiliania huxleyi* in mesocosm experiments. *Limnol. Oceanogr.*, **50**, 493–507.

Feely, R. A., Doney, S. C. and Cooley, S. R. (2009) Ocean acidification. Present conditions and future changes in a high-CO_2 world. *Oceanography*, **22**, 36–47.

Gärdes, A., Iversen, M. H., Grossart, H.-P. *et al.* (2011) Diatom-associated bacteria are required for aggregation of *Thalassiosira weissflogii*. *ISMEJ*, **5**, 436–445.

Gehlen, M., Gruber, N., Gangsto, R. *et al.* (2011) Biogeochemical consequences of ocean acidification and feedbacks to the earth system. In Gattuso, J. P. and Hansson, L. (eds), *Ocean Acidification*. Oxford University Press, Oxford, UK, pp 99–121.

Grossart, H. P., Simon, M. and Logan, B. E. (1997) Formation of macroscopic organic aggregates (lake snow) in a large lake: the significance of transparent exopolymer particles, phytoplankton, and zooplankton. *Limnol. Oceanogr.*, **42**, 1651–1659.

Hansen, H. P. and Koroleff, F. (1999) *Determination of Nutrients. Methods of Seawater Analysis*, 3rd edn. Grasshoff, K., Kremling, K. and Ehrhardt, M. (eds), Wiley, Weinheim.

Havenhand, J., Dupont, S. and Quinn, G. P. (2011) Design ocean acidification experiments to maximize inference. In Gattuso, J. -P. and Hansson, L. (eds), *Ocean Acidification*. Oxford University Press, Oxford, UK.

Hofmann, G. E., Smith, J. E., Johnson, K. S. *et al.* (2011) High-frequency dynamics of ocean pH: a multi-ecosystem comparison. *PLoS ONE*, **6**, 12.

Hoppe, H. -G. (1983) Significance of exoenzymatic activities in the ecology of brackish water – measurements by means of methylumbelliferyl-substrates. *Mar. Ecol. Prog Ser.*, **11**, 299–308.

Ittekkot, V., Brockmann, U., Michaelis, W. *et al.* (1981) Dissolved free and combined carbohydrates during a phytoplankton bloom in the northern North sea. *Mar. Ecol. Prog. Ser.*, **4**, 299–305.

Jackson, G. A. (1990) A model of the formation of marine algal flocs by physical coagulation processes. *Deep-Sea Res. A*, **37**, 1197–1211.

Joint, I., Doney, S. and Karl, D. (2011) Will ocean acidification affect marine microbes? *ISMEJ*, **5**, 1–7.

Kahl, L. A., Vardi, A. and Schofield, O. (2008) Effects of phytoplankton physiology on export flux. *Mar. Ecol. Prog. Ser.*, **354**, 3–19.

Kaehler, P. and Koeve, W. (2001) Marine dissolved organic matter: can its C:N ratio explain carbon overconsumption? *Deep-Sea Res. I*, **48**, 49–62.

Kim, J. M., Lee, K., Shin, K. *et al.* (2011) Shifts in biogenic carbon flow from particulate to dissolved forms under high carbon dioxide and warm ocean conditions. *Geophys. Res. Lett.*, **38**, doi:10.1029/2011GL047346

Kirchman, D. L., Meon, B., Ducklow, H. W. *et al.* (2001) Glucose fluxes and concentrations of dissolved combined neutral sugars

(polysaccharides) in the Ross Sea and Polar Front Zone. Antarctica. *Deep Sea Res, II*, **48**, 19–20.

Kroeker, K. J., Kordas, R. L., Crim, R. N. *et al*. (2010) Meta-analysis reveals negative yet variable effects of ocean acidification on marine organisms. *Ecol. Lett.*, **13**, 1419–1434.

Kulinski, K. and Pempkowiak, J. (2008) Dissolved organic carbon in the southern Baltic Sea: quantification of factors affecting its distribution. *Estuarine Coastal Shelf Sci.*, **78**, 38–44.

Lewis, E. L. (1980) The practical salinity scale 1978 and its antecedents. *IEEE J. Ocean Eng.*, **5**, 3–8.

Leppäranta, M. and Myrberg, K. (2009) *Physical Oceanography of the Baltic Sea*. Springer-Praxis Books in Geophysical Sciences.

Lindroth, P. and Mopper, K. (1979) High performance liquid chromatography determination of subpicomole amounts of amino acids by precolumn fluorescence derivatisation with OPA. *Anal. Chem.*, **51**, 1667–1674.

Liu, J. W., Weinbauer, M. G., Maier, C. *et al*. (2010) Effect of ocean acidification on microbial diversity and on microbe-driven biogeochemistry and ecosystem functioning. *Aquat. Microb. Ecol.*, **61**, 291–305.

Lueker, T. J., Dickson, A. G. and Keeling, C. D. (2000) Ocean pCO2 calculated from dissolved inorganic carbon, alkalinity, and equations for K1 and K2: validation based on laboratory measurements of CO2 in gas and seawater at equilibrium. *Mar. Chem.*, **70**, 105–119.

Mari, X. (2008) Does ocean acidification induce an upward flux of marine aggregates? *Biogeosciences*, **5**, 1023–1031.

Mari, X. and Robert, M. (2008) Metal induced variations of TEP sticking properties in the southwestern lagoon of New Caledonia. *Mar. Chem.*, **110**, 98–108.

Mari, X., Migon, C. and Nicolas, E. (2009) Reactivity of transparent exopolymeric particles: a key parameter of trace metal cycling in the lagoon of Noumea, New Caledonia. *Mar. Pollut. Bull.*, **58**, 1874–1879.

Mari, X., Torreton, J. P., Claire, B. T. T. *et al*. (2012) Aggregation dynamics along a salinity gradient in the Bach Dang estuary, North Vietnam. *Estuarine Coastal Shelf Sci.*, **96**, 151–158.

Mehrbach, C., Culberson, C. H., Hawley, J. E. *et al*. (1973) Measurements of the apparent dissociation constants of carbonic acid in seawater at atmospheric pressure. *Limnol. Oceanogr.*, **18**, 897–907.

Melzner, F., Thomsen, J., Koeve, W. *et al*. (2012) Future ocean acidification will be amplified by hypoxia in coastal habitats. *Mar. Biol.*, DOI:10.1007/s00227-012-1954-1.

Omstedt, A., Edman, M., Anderson, L. G. *et al*. (2010) Factors influencing the acid-base (pH) balance in the Baltic Sea: a sensitivity analysis. *Tellus B*, **62**, 280–295.

Omstedt, A., Gustafsson, E. and Wesslander, K. (2009) Modelling the uptake and release of carbon dioxide in the Baltic Sea surface water. *Cont. Shelf Res.*, **29**, 870–885.

Oschlies, A., Schulz, K. G., Riebesell, U. *et al*. (2008) Simulated 21st century's increase in oceanic suboxia by CO2-enhanced biotic carbon export. *Global Biogeochem. Cycles*, **22**, 1–10.

Passow, U. (2002) Transparent exopolymer particles (TEP) in aquatic environments. *Prog. Oceanogr.*, **55**, 287–333.

Passow, U. (2011) The abiotic formation of TEP under ocean acidification scenarios. *Mar. Chem.*, **129**, 72–80.

Passow, U. and Alldredge, A. L. (1995a) A dye-binding assay for the spectrophotometric measurement of transparent exopolymer particles (TEP) in the ocean. *Limnol. Oceanogr.*, **40**, 1326–1335.

Passow, U. and Alldredge, A. L. (1995b) Agggregation of a diatom bloom in a mesocosms—the role of transparent exopolymer particles (TEP). *Deep- Sea Res. II*, **4**, 99–109.

Passow, U., Shipe, R. F., Murray, A. *et al*. (2001) The origin of transparent exopolymer particles (TEP) and their role in the sedimentation of particulate matter. *Cont. Shelf Res.*, **21**, 327–346.

Piontek, J., Händel, N., de Bodt, C. *et al*. (2011) The utilization of polysaccharides by heterotrophic bacterioplankton in the Bay of Biscay (North Atlantic Ocean). *J. Plankton Res.*, **33**, 1719–1735.

Piontek, J., Lunau, M., Händel, N. *et al*. (2010) Acidification increases microbial polysaccharide degradation in the ocean. *Biogeosciences*, **7**, 1615–1624.

Qian, J. and Mopper, K. (1996) An automated, high performance, high temperature combustion dissolved organic carbon analyzer. *Anal. Chem.*, **68**, 3090–3097.

Riebesell, U., Czerny, J., von Bröckel, K. *et al*. (2013) Technical Note: a mobile sea-going mesocosm system—new opportunities for ocean change research. *Biogeosciences*, **10**, 1835–1847.

Riebesell, U., Schulz, K. G., Bellerby, R. G. J. *et al*. (2007) Enhanced biological carbon consumption in a high CO_2 ocean. *Nature*, **450**, 545–U510.

Riebesell, U. and Tortell, P. D. (2011) Effects of ocean acidification on pelagic organisms and ecosystems. In Gattuso, J.-P. and Hansson, L. (eds.), *Ocean Acidification*. Oxford University Press, Oxford, UK.

Sarmiento, J. L. and Gruber, N. (2006) *Ocean Biogeochemical Dynamics*. Princeton University press, Princeton, NJ, 526pp.

Schartau, M., Engel, A., Schröter, J. *et al*. (2007) Modelling carbon overconsumption and the formation of extracellular particulate organic carbon. *Biogeosciences*, **4**, 433–454.

Schulz, K. G. and Riebesell, U. (2012) Diurnal changes in seawater carbonate chemistry speciation at increasing atmospheric carbon dioxide. *Mar. Biol.*, doi:10.1007/s00227-012-1965-y.

Sharp, J. H. (1974) Improved analysis for 'particulate' organic carbon and nitrogen from seawater. *Limnol. Oceanogr.*, **19**, 984–989.

Simon, M., Grossart, H. P., Schweitzer, B. *et al*. (2002) Microbial ecology of organic aggregates in aquatic ecosystems. *Aquat. Microb. Ecol.*, **28**, 175–211.

Skoog, A. and Benner, R. (1997) Aldoses in various size fractions of marine organic matter. Implications for carbon cycling. *Limnol. Oceanogr.*, **42**, 1803–1813.

Smith, D. C., Simon, M., Alldredge, A. L. *et al*. (1992) Intense hydrolytic enzyme activity on marine aggregates and implications for rapid particle dissolution. *Nature*, **359**, 139–142.

Stoderegger, K. E. and Herndl, G. J. (1999) Production of exopolymer particles by marine bacterioplankton under contrasting turbulence conditions. *Mar. Ecol. Prog. Ser.*, **189**, 9–16.

Thingstad, T. F., Hagstrom, A. and Rassoulzadegan, F. (1997) Accumulation of degradable DOC in surface waters: is it caused by a malfunctioning microbial loop? *Limnol. Oceanogr.*, **42**, 398–404.

Thornton, D. C. O. (2009) Effect of low pH on carbohydrate production by a marine planktonic diatom (*Chaetoceros muelleri*). *Res. Lett. Ecol.*, doi:10.1155/2009/105901.

Welschmeyer, N. A. (1994) Fluometric analysis of chlorophyll *a* in the presence of chlorophyll *b* and pheopigments. *Limnol. Oceanogr.*, **39**, 1985–1992.

Williams, P. J. le B. (1995) Evidence for the seasonal accumulation of carbon-rich dissolved organic material, its scale in comparison with changes in particulate material and the consequential effect on net C/N assimilation ratios. *Mar. Chem.*, **51**, 17–29.